

Location of Methanol on the S₂ state Mn cluster in Photosystem II Studied by Proton Matrix Electron Nuclear Double Resonance

*Hiroki Nagashima and Hiroyuki Mino**

Division of Material Science, Graduate School of Science, Nagoya University, Furo-cho,
Chikusa-ku, 464-8602, Nagoya, Aichi, Japan.

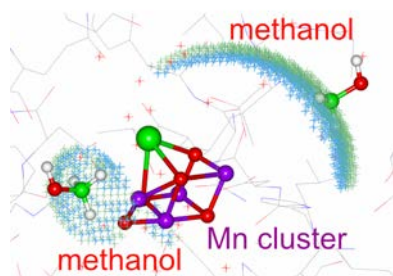
Corresponding Author

*E-mail: mino@bio.phys.nagoya-u.ac.jp

Abstract

Proton matrix electron nuclear double resonance (ENDOR) spectroscopy was performed in order to specify the location of the methanol molecule near the manganese cluster in photosystem II. Comparison of the ENDOR spectra in the presence of CH_3OH and CD_3OH revealed two pairs of hyperfine couplings, 1.2 MHz for A_{\perp} and 2.5 MHz for A_{\parallel} , arising from the methyl group in methanol. Based on the crystal structure, the possible location of methanol close to the manganese cluster was discussed.

TOC GRAPHICS



KEYWORDS photosystem II, manganese cluster, ENDOR, EPR, oxygen evolution

Oxidation of water in plants and cyanobacteria is catalyzed by the Mn cluster (Mn_4CaO_5) in the photosystem II (PS II) protein complex. The Mn cluster has five different redox states called S_n ($n = 0-4$), where the S_n state advances to the S_{n+1} state by oxidation. The S_4 state is the highest oxidized state and immediately reverts to the lowest oxidized S_0 state with the evolution of molecular oxygen¹⁻⁴. Crystal structure analysis of the PS II succeeded with a high resolution of $< 2 \text{ \AA}$ ⁵⁻⁷. The crystal structure revealed the location of the Mn_4CaO_5 cluster, positions of coordinated water molecules, W1-W4, (Fig. 1), surrounding amino acid residues, positions of the two chloride ions, and the hydrogen-bond pathway from the Mn cluster to outside of PS II.

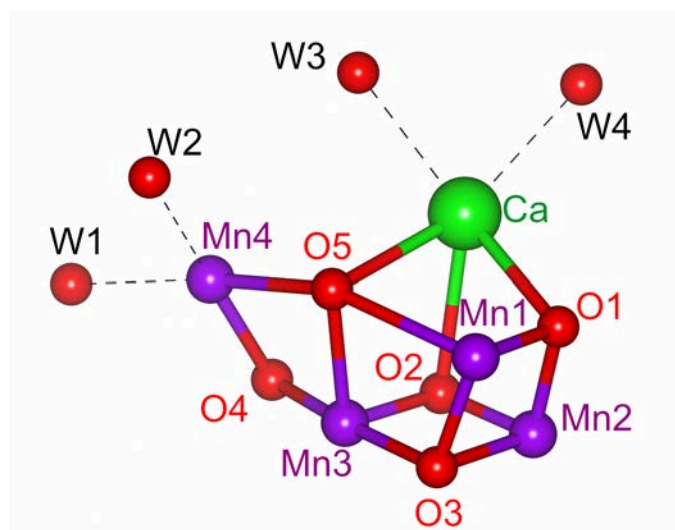


Fig. 1 The X-ray crystal structure of the Mn cluster (PDB ID 4UB6).

Methanol affects the magnetic structure of the manganese cluster, and has been proposed to bind to one or more of the Mn ions directly⁸⁻¹³. Although methanol seems to be competing with the water molecules, it does not inhibit the water oxidation activity of the Mn cluster at concentrations less than 3 M, above which the oxygen evolution activity decreased by 10%¹⁴. Methanol inhibits water oxidation activity at

concentrations higher than 5 M. The decrease in the evolution of oxygen in the presence of methanol is explained by the increase in the mishit probability of the S-state transitions in the range of 0–10% (v/v)⁸.

Electron paramagnetic resonance (EPR) spectroscopy characterizes the magnetic structure and chemical properties of the Mn cluster. In the S₂ state, methanol affects the balance of the g = 4 and g = 2 EPR signal intensities, ascribed to the equilibrium of isomers of the Mn cluster. This effect is much smaller in cyanobacteria (*T. elongatus*) than in spinach⁹. Methanol causes a narrowing of the S₂ EPR multiline signal, ascribed to the modification of the ⁵⁵Mn(III) hyperfine coupling anisotropy⁹. The effect of methanol on the magnetic structure and oxygen-evolving activity might be a clue towards identifying the positions of the substrates and the S-state transition mechanisms. Previous electron spin echo envelope modulation (ESEEM) studies suggested that methanol is bound to the Mn ion directly^{10, 14}. On the other hand, ¹³C-pulsed ENDOR indicates that the methanol is located at a more distant site such as the W3 water, or another water site that is close to the μ-oxo, O1 or O4¹⁵.

We have previously reported proton matrix ENDOR of the S₂ state multiline. Immobilized protons around the manganese cluster can be detected by continuous wave (CW) ENDOR with high spectral resolution¹⁶. The 6-7 pairs of proton signals, assigned to W1-W4 water protons, have been detected.

Fig. 2 shows the EPR spectra of the S₂ state PS II in the presence of CH₃OH and CD₃OH. The S₂ state multiline signals were detected around g = 2 in both samples. In the presence of methanol, the g = 4 signal was not observed and the amplitude of the g = 2 multiline signal doubled¹³. Fig. 3 shows the proton matrix ENDOR spectra of the S₂

state PS II in the presence of CH₃OH and CD₃OH. In both spectra, at least six pairs of ENDOR signals are detected and labeled as aa'-ff'¹⁶. ⁵⁵Mn ENDOR gave the different hyperfine parameters in the range of 0-10% depending on Mn in the presence and absence of CH₃OH⁹, however, the effect to the proton ENDOR was limited within spectral resolution. The differences in the samples would be averaged within linewidth, where the ¹H-ENDOR separation is made up with the summation between the protons and the projections of four Mn in the disordered orientation.

The line shape is similar to that of untreated PS II^{16, 17}, indicating that methanol does not replace the water molecules, previously assigned as the protons of W1-W4. At a glance, there are no spectral differences between the samples containing CH₃OH and CD₃OH, indicating that methanol does not affect the hydrogen-bond networks surrounding the W1-W4 site. However, some broadenings around the peaks e₁e₁' and e₂e₂' were observed, which is absent in the presence of CD₃OD. Fig. 3C shows the differential spectra in the presence of CH₃OH and CD₃OH, and the corresponding symmetrized spectra (Fig. 3D). ENDOR spectra of CH₃OH and CD₃OH were normalized by the region of narrow components (bb'-ff' peaks). In the subtracted spectra (Fig. 3C), two pairs of broad ENDOR signals (m₁m₁' and m₂m₂') were remained and ascribed to the methanol molecules (Fig. 3C and D). The m₁m₁' and m₂m₂' signals had hyperfine separations of 1.2 MHz and 2.5 MHz, and were assigned to A_⊥ and A_∥ with the axial symmetry, respectively. The linewidth of the m₁m₁' signal was approximately 0.2 MHz, which is larger than the other peaks (bb'-dd'). The linewidth is made up with the summation of intrinsic linewidth (Δ_{int}) and FM depth (Δ_{FM})¹⁶. The observed linewidth (Δ_{obs}) is estimated as $(\Delta_{\text{int}}^2 + \Delta_{\text{FM}}^2)^{1/2}$. Considering that the linewidth

(Δ_{int}) is ascribed to the distance distribution of the detected proton signals, it was estimated to be $< 0.1 \text{ \AA}$ for the bb' - dd' peaks¹⁶, and 0.24 \AA for the m_1m_1' peaks. These results show that methanol is immobilized, but not directly bound to the manganese cluster such as W1-W4.

Assuming the point dipole approximation, the distances between Mn and the protons was estimated to be 4.2 \AA . In reality, the electronic spin is distributed over the Mn cluster. The spin density distributions have been estimated by pulsed electron-electron double resonance (PELDOR), ^{55}Mn -ENDOR, and density functional theory (DFT) calculations as the projection factors¹⁸⁻²⁰. In these results, the spin projection of Mn1 is approximately 2, and the other Mn are close to 1²¹. When we simply evaluate the distance between the nuclei and the closest Mn ion as a point dipole approximation, the distance for Mn1 was calculated as 5.2 \AA .

Including the spin projection factors, the hyperfine couplings were calculated by the following equation:

$$A_{aniso} = \sum_{i=1}^4 \frac{\rho_i \mu_0 g \beta g_n \beta_n}{4\pi h} \frac{1-3\cos\theta_i}{R_i^3} \quad (1)$$

where g , β , g_n , and β_n are the g -factors and Bohr magnetons for the electron and nuclei, respectively. Further, h is the Planck constant, μ_0 is the vacuum permeability, θ is the angle between the R vector and the external magnetic field, ρ_i is the spin projection on the i^{th} Mn, and $R_i(x_i, y_i, z_i)$ is the distance between the nuclei and i^{th} Mn. After diagonalization, this equation is expressed by three eigenvalues, $A_{x,y,z}$, in the tensor form:

$$A_{aniso} = \begin{pmatrix} A_x & 0 & 0 \\ 0 & A_y & 0 \\ 0 & 0 & A_z \end{pmatrix} \quad (2)$$

$$\eta = \frac{A_x - A_y}{A_z} \quad (3)$$

$$T = \frac{A_z}{2} \quad (4)$$

where η is the rhombic factor and T is the amplitude of the dipolar hyperfine coupling.

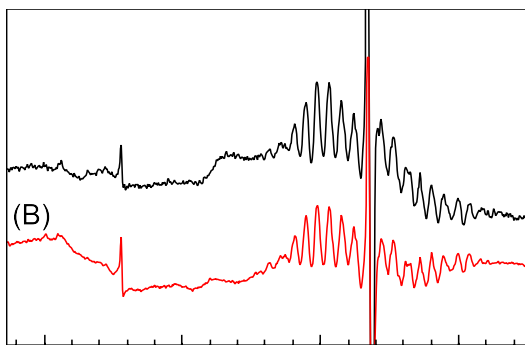


Fig. 2 EPR spectra of the S_2 state in PS II in the presence of (A) CH_3OH and (B) CD_3OH . Measurement conditions: microwave frequency, 9.44 GHz; microwave power, 0.2 mW; modulation amplitude, 0.8 mT; temperature, 6 K.

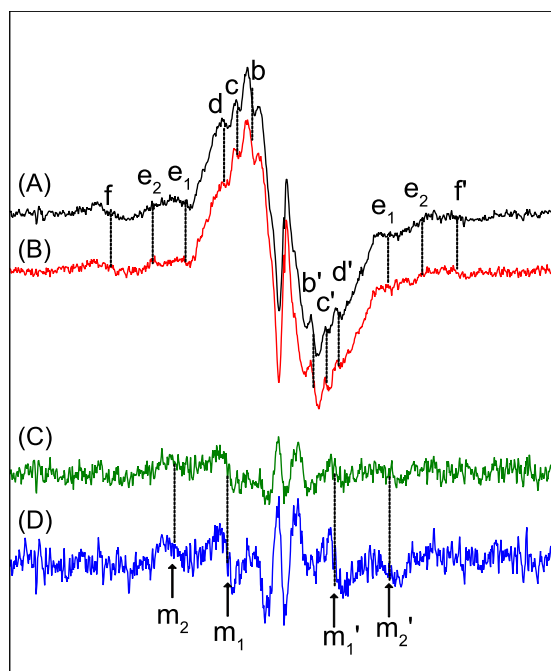


Fig. 3 ENDOR spectra of the S_2 state in PS II in the presence of (A) CH_3OH and (B) CD_3OH . (C) the subtraction of spectrum (B) from (A). (D) symmetrized spectrum (C). Measurement conditions: microwave frequency, 9.44 GHz; microwave power, 0.8 mW; magnetic field, 328.2 mT; FM modulation, 12.5 kHz; modulation depth, 0.2 MHz.

Oyala et al. showed that the hyperfine couplings of ^{13}C were $A_{\text{iso}} = 0.05 \pm 0.02$ MHz and $A_{\text{aniso}} = 0.27 \pm 0.05$ MHz, and suggested that methanol was displacing the Ca^{2+} ligand, W3. In addition, the water molecules, which are likely to form hydrogen bonds to the cluster through μ -oxo bridges, O1 or O4, were also suggested as the alternative displaced sites¹⁵. In contrast, Åhrling et al. have reported three hyperfine couplings for deuterons of the methyl group ($\text{CD}_3\text{-OH}$) as 0.64 MHz (one deuteron) and 0.39 MHz (for two deuterons)¹⁰. They suggested that CD_3OH is located at distances close enough for methanol to be a direct Mn ligand. The deuteron hyperfine couplings were converted to the proton hyperfine couplings using nuclear magnetic constants, yielding values of 4.17 and 2.54 MHz. These obtained values of

hyperfine couplings do not fit the ^1H -ENDOR results. The inconsistency would be caused by some disadvantages of deuteron ESEEM analysis: (1) the quadrupole couplings are assumed as zero¹⁰ or 0.22 MHz¹⁴, (2) ^{14}N signals overlap with ^2H -ESEEM, (3) the spectral resolution was too low to distinguish the three deuteron signals.

The present CW-ENDOR results support the ^{13}C -ENDOR results¹⁵. The methyl group is located at distances of 4–5 Å from the Mn cluster. If the methyl group is close to Mn4, where the spin projection is close to 1, the Mn-H distances are estimated to be 4.2 Å. If methylene protons are located at a distance of 4.2 Å from Mn, the distance of the corresponding ^{13}C atom would be 3.7 or 4.4 Å from the Mn cluster. Since a distance of 3.7 Å is too low and inconsistent with the ^{13}C -pulsed ENDOR¹⁵, the Mn-C distance is likely 4.4 Å. If the closest Mn is Mn1, the Mn-H distances are estimated to be 5.2 Å, where the spin projection is close to 2. Considering the structure of CH_3OH , the Mn-C distances are estimated at 5.4–5.5 Å or 4.7–4.8 Å. The Mn-C distance of 4.7–4.8 Å is a bit low compared to the ^{13}C -pulsed ENDOR results. In any case, the Mn-H distances are shorter than the Mn-C distances, indicating that the hydroxo group of the methanol is located farther than the methyl group. Methanol does not actually interact directly with the Mn cluster but remotely via the hydrogen-bond network or backbones of amino acid residues.

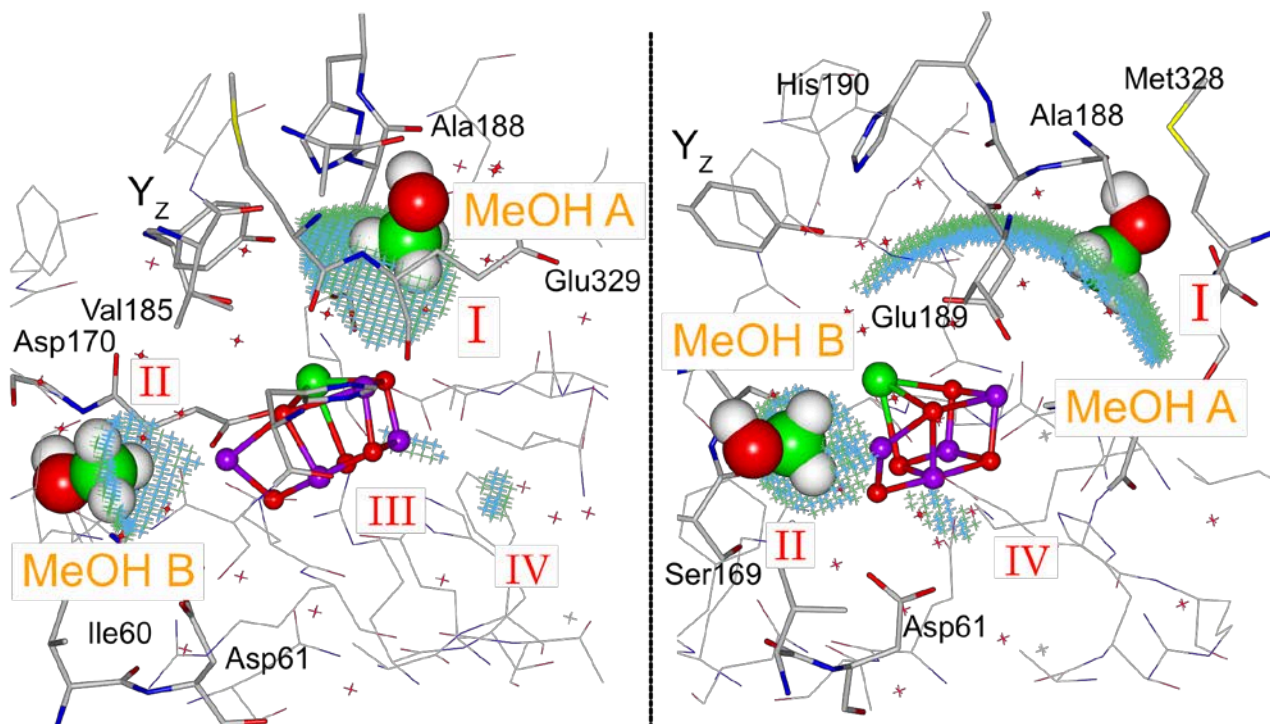


Fig. 4 Possible location of the methanol close to the Mn cluster. Proton positions with axial parameter $\eta < 0.1$ and 1.1–1.3 MHz hyperfine couplings are shown as a light blue mesh surface. ^{13}C positions with axial parameter $\eta < 0.1$ and 0.22–0.32 MHz hyperfine couplings are shown in green. Amino acid residues within an 8 Å radius from the Mn cluster are drawn with thin sticks. Amino acid residues within a 3 Å radius from the areas I and II are drawn with bold sticks. Methanol molecules A and B were introduced on the surfaces of areas I and II, respectively. Areas III and IV are too small to introduce methanol molecules. Methanol molecules A and B are hydrogen-bonded to Gly171 and Ala188, respectively.

Fig. 4 shows the isosurface plots of the hyperfine couplings of protons and carbon atoms. Spin projections (1.97, -1.20, 1.19, -0.96) for Mn1–4, determined from the PELDOR experiments²⁰, were employed to calculate the hyperfine couplings. Using the different spin projections in DFT calculations^{15, 22}, the obtained results are qualitatively equivalent (data not shown). In this analysis, only ‘axial’ locations under the condition of rhombicity ($\eta < 0.1$) were picked up. If the rhombicity was neglected, the obtained picture would be compatible to that drawn by Oyala et al¹⁵. The blue and green surfaces show the possible locations of the methyl group of the methanol. There are four

different regions. Two areas labeled as III and IV in Fig. 4, close to Mn2 and O2, were excluded as they were too small. The possible location of the methanol molecule is limited to the regions close to Mn1, (area I) and Mn4 (area II). The width of area I (located on Glu189) is approximately 4.0 Å, perpendicular to the arc, and 10 Å along the arc. Besides, area I is surrounded by amino acids and water within 3 Å, labeled Ala188, Glu329, Met328, His332, His190, Tyr161, HOH568, HOH554, HOH503, HOH570, HOH571. Area II is not located on the other atoms. The width of area II is ~3.5 Å, and the surrounding amino acids and water within 3 Å are labeled as Asp170, Ser169, Asp61, Ile60, HOH556, HOH608, HOH560, HOH607, HOH557, and HOH575 (labels taken from PDB 4UB6). The Glu189 and His332 amino acids from area I and Asp170 from area II are directly connected to the Mn cluster.

The corresponding areas for ^{13}C in the methyl group were overlapped in Fig. 4 with the mesh. Since methanol does not interact with the Mn cluster directly, it could influence the chemical properties of the Mn cluster through hydrogen bonds. The hydrogen-bond network through W3 has been proposed as the proton transfer path. Recently, the hydrogen-bond network close to O4 has also been suggested for the function of oxygen evolution^{23, 24}. Retegan and Pantazis suggested that the location of the methanol was close to O4²². However, our possible methanol sites shown in Fig. 4 do not fit to the O4 or W3 site.

Insertion of methanol close to these amino acids might result in some modification of the structure of the Mn cluster. Recent DFT calculations suggested that the S_2 state has two different isomers, which are called the ‘open cubane’ and ‘closed cubane’ states. The S_2 multiline signal is attributed to the $S = 1/2$ ‘open cubane’ state in which O5 is connected to Mn4, Mn3, and Ca; Mn1 is in the five coordinated trivalent state. The $g = 4$ signal is attributed to the $S = 5/2$ ‘closed cubane’ state, where O5 is coordinated to Mn1 and the ‘closed cubane’ structure is composed of Mn1–3 and Ca. The chloride anion, located within ~7 Å from the Mn cluster, also affects the equilibrium. The

cyanobacteria *T. vulcanus*, which has a larger Δ than spinach⁹, exhibits no $g = 4$ signals in the absence of methanol.

If methanol is located in area I, close to Mn1, the structural modification via the amino acids surrounding Mn1 might cause the modification on the hyperfine anisotropy of the Mn1⁹. The interaction with the hydrogen-bonding network via W4 and Y_Z located nearby would lower the reaction rate¹⁷. On the other hand, modification of the spin structure is not necessary to be located close to Mn1 in the coupled spin system. The disruption of the hydrogen-bond network surrounding the Mn cluster would also cause the modification in the amplitude of Δ . The area II, close to Mn4, would disrupt the whole hydrogen bond structure and the equilibrium would be modified. In addition, Ser169 is in close proximity to Asn87, which is the only amino acid around the Mn cluster that differs between higher plants and cyanobacteria; the Asn87 in cyanobacteria is replaced by alanine in spinach. If the difference is ascribed to the stability of the isomer multiline / $g = 4$ through the hydrogen-bonded network, then the insertion of the methanol molecule in area II would disturb the network. It should be noted that there is CP43-Arg357 between Asn87 and the Mn cluster. Arg357 is a conserved key residue in the oxygen evolving activity. The difference of Asn87 site might be not so crucial since Asn87 is actually not a strong H-bond partner. The conservation of Arg357 would compensate for such a tiny difference.

The detected methanol site is corresponded to the previous report¹⁵. However, the second methanol site may interact to the Mn cluster¹¹. There are two possibilities: (1) two methanol molecules are located in the areas I and II, (2) the second methanol molecule is undetectable because it is located in very high mobility site, or in distant site (over $\sim 5\text{-}6$ Å, the limit of the ENDOR detection).

The methanol molecule is located in a stable position relative to the Mn cluster with a mobility of 0.2 Å. Tentatively, the methanol molecules (labeled as MeOH A and B) were introduced into

both areas I and II, as illustrated in Fig. 4. We assumed that the methanol molecules form a hydrogen bond with Ala188 in area I and Gly171 in area II. In area I, a position close to Y_Z and His190 could also be considered, however, the other surrounding amino-acids are packed closely. For more precise discussions, theoretical calculations, such as QM/MM and MD, would help to evaluate the stability of methanol in these sites.

Experimental Methods

The PS II membranes were prepared as described previously^{25, 26}, and suspended in a buffer containing 0.4 M sucrose, 20 mM NaCl, 0.5 mM EDTA, and 20 mM Mes/NaOH (pH6.5). Methanol (CH₃OH or CD₃OD) of 3% (v/v) was added to the buffer. The PS II membranes were transferred into quartz EPR tube, and illuminated in an ethanol bath by a 500 W tungsten lamp, at 200 K.

EPR and ENDOR were measured by a Bruker ESP300E instrument equipped with a homemade ENDOR cavity. An Oxford ESR900 cryostat was used for the measurements.

ACKNOWLEDGMENT

This work was supported by a Program for Leading Graduate Schools “Integrative Graduate Education and Research in Green Natural Sciences”, MEXT, Japan and Grant-in-Aid for JSPS Fellows No. 26011113 to H.N. and a MEXT/JSPS Grant-in-Aid for Exploratory Research No. 26620003 to H. M.

REFERENCES

- (1) McEvoy, J. P.; Brudvig, G. W., Water-splitting chemistry of photosystem II. *Chem Rev* **2006**, *106*, 4455-4483.
- (2) Nelson, N.; Yocum, C. F., Structure and function of photosystems I and II. *Annu Rev Plant biol*

2006, 57, 521-565.

- (3) Yocum, C. F., The calcium and chloride requirements of the O₂ evolving complex. *Coordin Chem Rev* **2008**, 252, 296-305.
- (4) Cox, N.; Pantazis, D. A.; Neese, F.; Lubitz, W., Biological water oxidation. *Acc Chem Res* **2013**, 46, 1588-1596.
- (5) Umena, Y.; Kawakami, K.; Shen, J.-R.; Kamiya, N., Crystal structure of oxygen-evolving photosystem II at a resolution of 1.9 Å. *Nature* **2011**, 473, 55-60.
- (6) Suga, M., *et al.*, Native structure of photosystem II at 1.95 Å resolution viewed by femtosecond X-ray pulses. *Nature* **2015**, 517, 99-103.
- (7) Young, I. D., *et al.*, Structure of photosystem II and substrate binding at room temperature. *Nature* **2016**, 540, 453-457.
- (8) Nöring, B.; Shevela, D.; Renger, G.; Messinger, J., Effects of methanol on the S₁-state transitions in photosynthetic water-splitting. *Photosynth Res* **2008**, 98, 251-260.
- (9) Su, J.-H., *et al.*, The electronic structures of the S₂ states of the oxygen-evolving complexes of photosystem II in plants and cyanobacteria in the presence and absence of methanol. *Biochem Biophys Acta* **2011**, 1807, 829-840.
- (10) Åhrling, K. A.; Evans, M. C. W.; Nugent, J. H. A.; Ball, R. J.; Pace, R. J., ESEEM studies of substrate water and small alcohol binding to the oxygen-evolving complex of photosystem II during functional turnover. *Biochemistry* **2006**, 45, 7069-7082.
- (11) Sjöholm, J.; Chen, G.; Ho, F.; Mamedov, F.; Styring, S., Split electron paramagnetic resonance signal induction in photosystem II suggests two binding sites in the S₂ state for the substrate analogue methanol. *Biochemistry* **2013**, 52, 3669-3677.
- (12) Su, J.-H.; Havelius, K. G.; Mamedov, F.; Ho, F. M.; Styring, S., Split EPR signals from photosystem II are modified by methanol, reflecting S state-dependent binding and alterations in the magnetic coupling in the CaMn₄ cluster. *Biochemistry* **2006**, 45, 7617-7627.
- (13) Deák, Z.; Peterson, S.; Geijer, P.; Åhrling, K. A.; Styring, S., Methanol modification of the electron paramagnetic resonance signals from the S₀ and S₂ states of the water-oxidizing complex of Photosystem II. *Biochem Biophys Acta* **1999**, 1412, 240-249.
- (14) Force, D. A.; Randall, D. W.; Lorigan, G. A.; Clemens, K. L.; Britt, R. D., ESEEM Studies of Alcohol Binding to the Manganese Cluster of the Oxygen Evolving Complex of Photosystem II. *J Am Chem Soc* **1998**, 120, 13321-13333.
- (15) Oyala, P. H.; Stich, T. A.; Stull, J. A.; Yu, F. T.; Pecoraro, V. L.; Britt, R. D., Pulse electron paramagnetic resonance studies of the interaction of methanol with the S₂ state of the

Mn₄O₅Ca cluster of photosystem II. *Biochemistry* **2014**, *53*, 7914-7928.

- (16) Nagashima, H.; Mino, H., Highly resolved proton matrix ENDOR of oriented photosystem II membranes in the S₂ state. *Biochem Biophys Acta* **2013**, *1827*, 1165-1173.
- (17) Nagashima, H.; Nakajima, Y.; Shen, J.-R.; Mino, H., Proton matrix ENDOR studies on Ca²⁺-depleted and Sr²⁺-substituted manganese cluster in photosystem II. *J Biol Chem* **2015**, *290*, 28166-28174.
- (18) Peloquin, J. M.; Campbell, K. A.; Randall, D. W.; Evanchik, M. A.; Pecoraro, V. L.; Armstrong, W. H.; Britt, R. D., ⁵⁵Mn ENDOR of the S₂-state multiline EPR signal of photosystem II: Implications on the structure of the tetranuclear Mn cluster. *J Am Chem Soc* **2000**, *122*, 10926-10942.
- (19) Ames, W. M.; Pantazis, D. A.; Krewald, V.; Cox, N.; Messinger, J.; Lubitz, W.; Neese, F., Theoretical evaluation of structural models of the S₂ state in the oxygen evolving complex of Photosystem II: protonation states and magnetic interactions. *J Am Chem Soc* **2011**, *133*, 19743-19757.
- (20) Asada, M.; Nagashima, H.; Koua, F. H. M.; Shen, J.-R.; Kawamori, A.; Mino, H., Electronic structure of S₂ state of the oxygen-evolving complex of photosystem II studied by PELDOR. *Biochem Biophys Acta* **2013**, *1827*, 438-445.
- (21) Peloquin, J. M.; Britt, R. D., EPR/ENDOR characterization of the physical and electronic structure of the OEC Mn cluster. *Biochem Biophys Acta* **2001**, *1503*, 96-111.
- (22) Retegan, M.; Pantazis, D. A., Interaction of methanol with the oxygen-evolving complex: atomistic models, channel identification, species dependence, and mechanistic implications. *Chem Sci* **2016**, *7*, 6463-6476.
- (23) Retegan, M.; Krewald, V.; Mamedov, F.; Neese, F.; Lubitz, W.; Cox, N.; Pantazis, D. A., A five-coordinate Mn(IV) intermediate in biological water oxidation: spectroscopic signature and a pivot mechanism for water binding. *Chem Sci* **2016**, *7*, 72-84.
- (24) Saito, K.; Rutherford, A. W.; Ishikita, H., Energetics of proton release on the first oxidation step in the water-oxidizing enzyme. *Nat Commun* **2015**, *6*, 8488.
- (25) Berthold, D. A.; Babcock, G. T.; Yocum, C. F., A highly resolved, oxygen-evolving photosystem II preparation from spinach thylakoid membranes. *FEBS Lett* **1981**, *134*, 231-234.
- (26) Ono, T.; Inoue, Y., Effects of removal and reconstitution of the extrinsic 33, 24 and 16 kDa proteins on flash oxygen yield in Photosystem II particles. *Biochem Biophys Acta* **1986**, *850*, 380-389.